Full Paper

Propellants, Explosives, Pyrotechnics

DOI: 10.1002/prep.201900217

X-ray Phase Contrast Imaging of the Impact of Multiple HMX Particles in a Polymeric Matrix

Nicholas E. Kerschen,[a] Jonathan D. Drake,*[b] Christian J. Sorensen,[a] Zherui Guo,[b] Jesus O. Mares,[a] Kamel Fezzaa,[c] Tao Sun,[c] Steven F. Son,[a, b] and Weinong W. Chen[a, b, d]

Abstract: The initiation of high explosives (HEs) under shock loading lacks a comprehensive understanding: particularly at the particle scale. One common explanation is the hot spot theory, which suggests that energy in the material resulting from the impact event is localized in a small area causing an increase in temperature that can lead to ignition. This study focuses on the response of HMX particles (a common HE) within a polymer matrix (Sylgard-184®), a simplified example of a polymer-bound explosive (PBX). These PBXs consist of multiple HMX particles in a single polymer-bound sample. A light gas gun was used to load the samples at impact velocities above 400 m/s. The impact events were visualized using X-ray phase-contrast imaging (PCI) allowing real-time observation of the impact event. The experiment used two different types of samples (multi-particle and two crystals) and found evidence of cracking and debonding in both sample types. In addition, it was found that the multiple particle samples showed similar evidence of damage at lower velocities than that of single particle samples. This is an expected result as the multiple particles add additional interfaces for stress concentration and frictional heating.

Keywords: HMX · Impact · PCI · Reaction · Energetics

1 Introduction

The response of energetic materials under the impact, particularly when ignition occurs, is of great interest to military and civilian organizations. As munitions increase in energy potential, the need for those munitions to be insensitive (that is to have a low sensitivity) is vital [1–2]. While creating energetic materials with varying threshold energies for ignition is of some use, it is widely observed that energetic materials can ignite at energies lower than the desired threshold. On the particle level, it is not completely understood what mechanism or mechanisms lead to ignition providing a need for an investigation. While several mechanisms have been proposed, the most widely accepted is the hot spot theory.

Hot spot theory has been the dominating explanation for explosive detonation that occurs at insufficient energy levels for decades. This theory predicts that the necessary energy for ignition under impact loading comes from energy consolidation caused by damage and deformation. Essentially, some mechanisms (or combination of mechanisms) occur in the material that causes thermal energy to concentrate in a microscopic region of critical volume, allowing that particular region to reach ignition temperatures. The term came about after it became clear that energetic materials could be ignited at energy levels insufficient to raise the bulk material to the necessary temperature [3]. Upon the formation of the hot spot, it can either fail (not reach the critical energy), or react to form an ignition site in the energetic material [4]. These ignition sites do not necessarily mean that the bulk material will detonate, they can deflagrate (burn) or they can contribute to a growing shockwave that could lead to a larger reaction [5]. The end result of a hot spot is a factor of various chemical and physical properties and is subject to debate among many proposed hot spot mechanisms [4].

These debated interactions are wide-ranging including defect and pore interactions [6–9], particle-particle interactions [10,11], energy dissipation [12], and frictional heating [13–14]; however as this paper focuses on PBX samples with two or more HMX particles, the most relevant factor is the particle-particle interactions and frictional heating. Zhou *et al.* looked into the surface roughness and found that there is a "statistically significant" correlation between the surface quality and the shock sensitivity [1]. They discussed that shock sensitivity could be lessened by a smooth surface finish, changing the initiation pressure from 3.3 GPa

[a] *N. E. Kerschen, C. J. Sorensen, J. O. Mares, S. F. Son, W. W. Chen*
School of Mechanical Engineering, Purdue University, 585 Purdue Mall, West Lafayette, Indiana, 47907, USA
[b] *J. D. Drake, Z. Guo, S. F. Son, W. W. Chen*
School of Aeronautics and Astronautics, Purdue University, 701 West Stadium Avenue, West Lafayette, Indiana, 47907, USA
**e-mail: drake44@purdue.edu*
[c] *K. Fezzaa, T. Sun*
Argonne National Laboratory, 9700 Cass Avenue, Lemont, Illinois, 60439, USA
[d] *W. W. Chen*
School of Materials Engineering, Purdue University, 701 West Stadium Avenue, West Lafayette, Indiana, 47907, USA

to 3.9 GPa by merely changing the surface texture [1]. Furthermore, they also discussed the formation of hot spots at the interface of the energetic crystal and the polymer matrix [1].

Baer and Trott approached these concepts while looking at heterogeneous PBXs, a complex analysis [11]. Using Mesoscale modeling, they put together random HMX particles in a polymer binder and modeled them under varying impact conditions [11]. They started with inert HMX particles at an impact speed of 1000 m/s to study the thermomechanical behaviors (here the conditions surely would produce the energy necessary for reaction). They found that the stress fields within the material fluctuated significantly because of the varying surface interactions due to the heterogeneous nature of the subject [11]. With this in mind, they observed that much of the localization of thermal energy came from the collapsing of voids within PBX [11]. Once the reactivity of the particles was added back into the model, the results are as expected. Where the localization occurred in the inert model, the reaction occurs and causes even larger pressure fields in the sample [12].

Another proposed factor to the formation and growth of hot spots centers around frictional heating, specifically near cracks. Several studies on this phenomena were performed by Dienes starting with a paper published in 1984. This study focused on frictional hot spots as well as propellant sensitivity (solid propellants). Because of erratic detonation behavior in the propellants, they hypothesized that hot spot theory may provide insight [13], so they decided to look at several mechanisms including frictional heating [13]. Dienes predicted that the most influential mechanism would be the formation of hotspots due to frictional heating: a mechanism that starts by estimating the heating of a closed crack from interfacial sliding with the one-dimensional heat flow equation [13]. In a simplified scenario, Dienes states that the ignition will occur when the temperature reaches a point where the heat conduction cannot remove enough of the heat generated in the material, yet they note that because of the complexity of crack behavior, these conclusions are not near definitive [13].

This work continued in 2006 with another paper on the ignition of explosives due to crack mechanics. This study used a statistical approach to model the response of cracks under dynamic loading [14]. After running several different experiments through their model, it shows that the hot spot formation and growth near cracks due to shear forces proves to be a viable mechanism, as well as a good explanation for ignition in stress regimes too low for spherical void collapse to be a viable mechanism [14].

More recent technological advancements have made the direct observation of particles under high-speed impact possible using X-ray phase-contrast imaging (PCI) [15–20]. The study discussed in this paper builds upon previous work performed on similar samples, but with only one HMX particle contained in each PBX [15]. That work showed that with an increase in velocity more cracking and debonding occurred in the particles. The highest velocity, 445 m/s, showed noticeable expansion originating at the cracks, possibly the result of gas formation from the reaction. This study looks specifically at multiple HE particles placed in a polymer matrix. A typical PBX would consist of 80–95 % of the HE particles contained in the polymer matrix. These HE particles would be a production-grade, thus polycrystalline containing possible defects and voids. These defects and voids are prime locations for the formation of hot spots and increase the sensitivity of PBX [21–25].

The experiments reported in this paper were performed using PCI to observe single-stage gas-gun impacts on PBX samples consisting of HMX (octahydro-1,3,5,7-tetranitro-1,3,5,7-tretrazocine) particles in Sylgard-184®. These PBX samples are divided into two categories: multiple smaller production-grade particles packed together in the polymer matrix and two single crystals placed face to face in line with the impact direction. The former examines the more complex interactions of multiple particles, while the latter looks at a simplified picture of just two crystals to focus the examination on one interface.

2 Experimental Section

The samples used in this study are in two classes: multiple production particles and two single low defect crystals. The first class of samples was prepared using a petri dish mold. Here a thin (~1 mm) layer of Sylgard-184® doped with 0.25 wt% Fe_2O_3 (spherical, 44 microns) was poured into a Teflon® petri dish and placed in a vacuum to remove all air bubbles. Sylgard-184® has a number average molecular weight of 6,190 g/mol and a weight average molecular weight of 27,700 g/mol giving a polydispersity index (ratio of weight average to number average) of 4.47 [26]. The Fe_2O_3 helps to provide contrast between the matrix and particle while using PCI [27] and is added after the Sylgard-184® is mixed, but before curing. Next, the dish was placed in an oven to cure the polymer to provide a base for the HMX particles to sit on (~30 minutes at 100 °C). After this, 7–10 HMX production-grade particles (roughly spherical with diameters between 0.2-0.5 mm) were placed in the mold and covered with more Sylgard-184® with Fe_2O_3, placed in the vacuum to degas, and fully cured in the oven (~30 minutes at 100 °C). Finally, samples were cut out of the petri dish to match the geometry shown in Figure 1. This method allowed for multiple samples to be made at once, but not with much geometric repeatability.

For the two single crystals, each sample consisted of two HMX crystals placed in line to the impact directions (i.e. the first crystal is impacted first, followed by the second). These low defect HMX crystals were purified and crystallized at Purdue University resulting in single crystals, which were then cut down to a simplified geometry, in this case, creating a generally flat interface between the crystals, as well as a normal plane to the impact direction. Once the

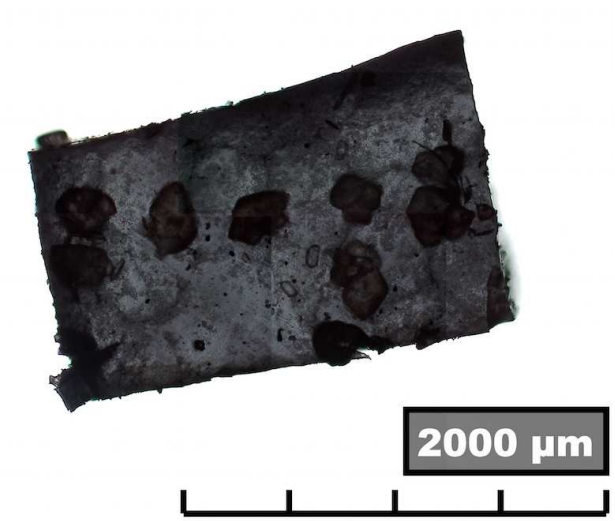

Figure 1. Multi-particle sample produced using the petri dish mold.

two HMX particles were prepared, they were again placed in a Sylgard-184® matrix doped with Fe_2O_3 (spherical, 77–100 microns). This time, this was achieved by using a different method with the Teflon™ mold seen in Figure 2. This mold provides a means to generate multiple samples with consistent size and geometry, 10.2 mm square with a height of 15.2 mm. The first crystal was precisely placed on the support to insure a flat plane for the next crystal to rest on. Sylgard-184® doped with Fe_2O_3 was filled to the top of the crystal and partially cured before placing the second crystal and repeating the process (~20 minutes at 100 °C).

Finally, the remainder of the mold was filled with the polymer before a final cure of 30 minutes at 100 °C. Additionally, before each curing step, the sample was placed in a vacuum chamber to degas, preventing any bubbles from forming in the sample.

The experimental work was performed using a gas gun with X-ray PCI to observe the dynamic deformation process in the sample as it was subjected to impact loading. The gas gun was a single-stage, smoothbore, light gas gun with a barrel length of 1.83 m and a bore diameter of 38.1 mm. At the time of these experiments, the maximum velocity of the gas gun was about 500 m/s. The impact event was captured using X-ray PCI provided at beamline 32-ID B at the Advanced Photon Source (APS) at Argonne National Laboratory [20]. The system allows the observation of phenomena not possible with standard optics due to the opaque nature of the samples, such as particle-matrix, and particle-particle interactions. X-rays pass into and out of the gun target chamber through a window to a scintillator placed in front of the camera lens, converting the X-rays to visible light [28]. Next, the light passes through an additional lens that magnifies the image (5x, or 10x) for better resolution. Finally, the light enters a Shimadzu HPV–X2 high-speed camera which records the impact event in real-time at 5 million frames per second. The schematic for this setup is seen in Figure 3.

There are only two major differences in the setup between the two classes of samples: the sabot and the triggering system. The multiple particle samples used a low-density polyurethane sabot formed in a cylindrical steel mold. A drill was then used to bore out part of the center of the cylinder and an aluminum impactor was added. The two single-crystal samples used a sabot that was machined out of Delrin® for precision and fitted with an aluminum impactor. This change was made to lower the tolerances on

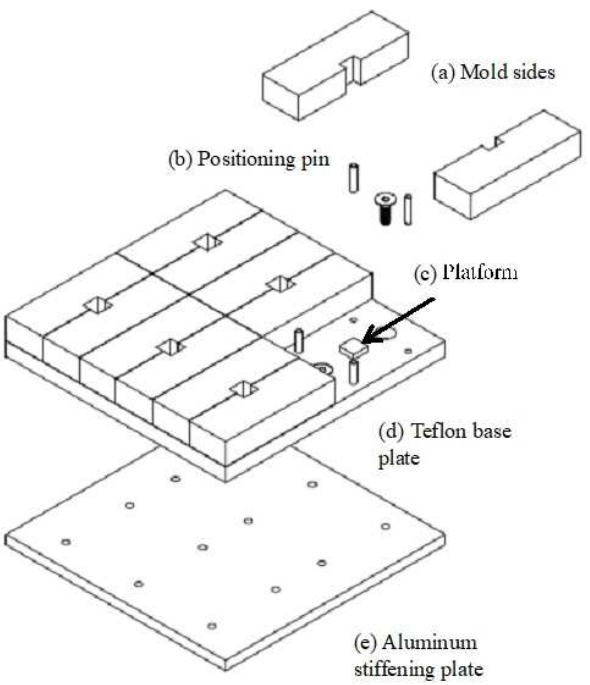

Figure 2. Exploded view of rectangular prism mold.

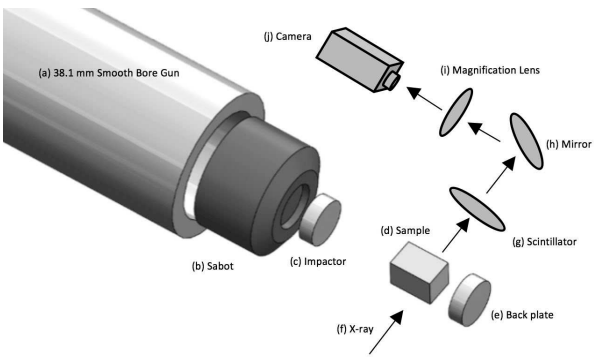

Figure 3. Gas gun setup schematic with an X-ray imaging system.

the sabot to allow for higher impact velocities. The triggering system also made a change between the groups of samples to precisely capture the impact event. Originally for the multiple particle samples, a 5 V laser was used to trigger the camera. This laser was placed ~25 mm in front of the sample and a delay generator was used to ensure the camera captured the impact event. This setup functioned well at lower velocities, however, the trigger became unreliable at higher velocities. The rest of the experiments were triggered using shorting pins, two wires that completed a circuit when connected by the impactor. These would be placed just behind the face of the sample to ensure clean contact with the sample surface. When connected, they would complete a capacitor circuit and trigger the camera.

The only additional change between experiments was slight variances in the delay settings for the camera and X-ray shutters. Throughout the study, an oscilloscope was used to find the function time (time between firing signal and camera trigger) to provide the best window for capturing the X-ray PCI images. The sample setup with the shorting pins can be seen in Figure 4.

3 Results and Discussion

Again, two different types of multi-particle samples were used in this study: multi-particle and two single crystals. These multi-particle samples are of interest as stress concentration and frictional heating at the interfaces are considered possible sources of hot spot formation [23–25]. It should be noted that X-ray PCI differs from a conventional X-ray image in that the measurement is a change in the X-ray phase due to the refractive index of the material, not attenuation of the X-ray [17]. The measurement of the X-ray phase is more sensitive to changes in density and thickness, allowing for better resolution of structural details in the material [29]. This makes PCI a great tool for observing cracks and opening interfaces in the HMX particles and crystals. These features appear lighter in color in the gray scale images as the X-rays encounter the less dense medium. PCI also results in a two-dimensional image of a three-dimensional object which can make the image difficult to interpret. It can be helpful to closely study the initial image (before impact) to note the changes as the impact loading occurs. These features are also better categorized when all the images can be viewed together in sequence. Arrows have been added to help point out these features.

The first two samples, figures 5 and 6, contain the production-grade multi-particle samples. The initial frame in each Figure shows the sample before impact, pointing out the placement of the particles. In Figure 5 (420 m/s), the second frame (t = 5.0 μs) shows the initial damage that occurs when the compressive wave reaches the particles in

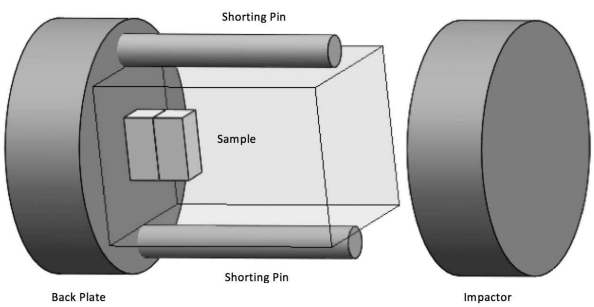

Figure 4. Trigger Pin setup for two crystal samples.

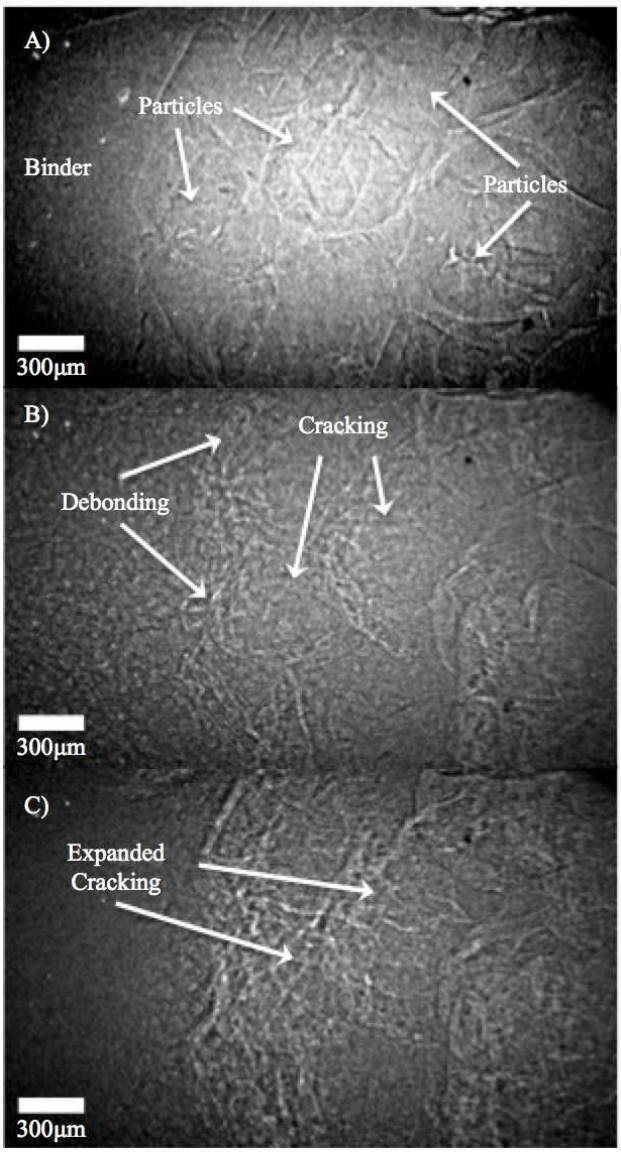

Figure 5. Image sequence of production HMX impacted at 420 m/s at A) 0 μs, B) 5.0 μs, and C) 6.5 μs.

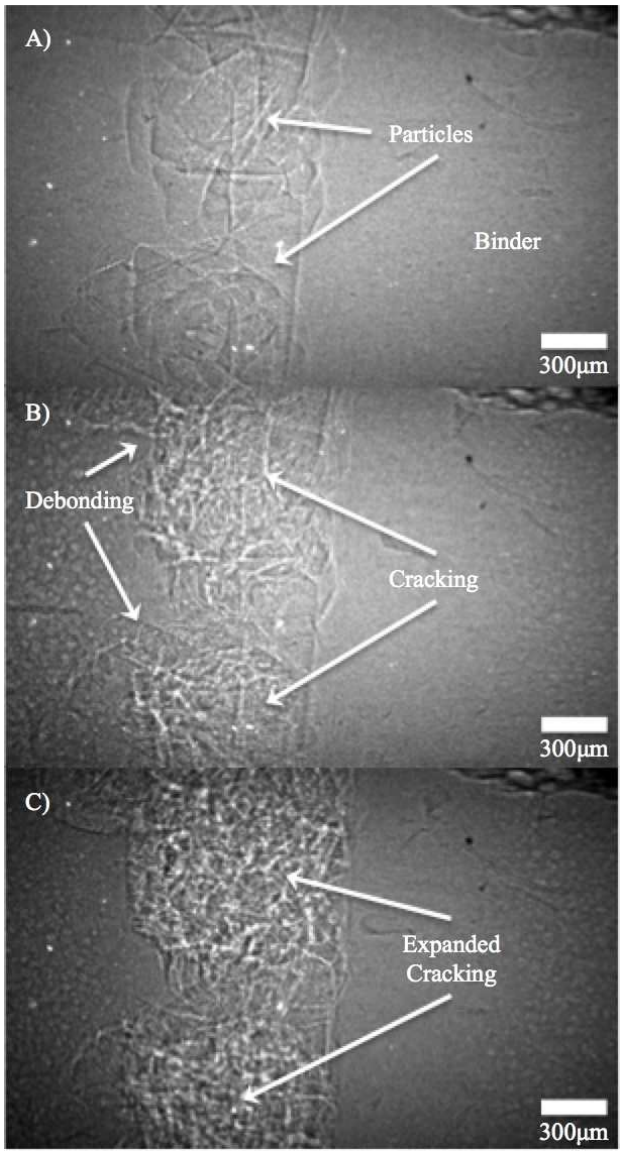

Figure 6. Image sequence of production HMX impacted at 429 m/s at A) 0 μs, B) 4.0 μs, and C) 8.5 μs.

the sample. A network of lighter colored lines forms on each of the particles, indicating either cracking in the particles, or open interfaces due to debonding with the matrix. These lines initially focus around the outer edge of the particles but begin to spread inward. Some of the lines are curved, likely indicating the latter explanation, however many are straight and appear to be cracks in the HMX particles. The third frame (t = 6.5 μs) shows the maximum expansion of this network before the sabot enters the frame and removes the sample from the viewing window. By this point, the lines have opened further and spread throughout the full volume of each particle. This behavior is mirrored in Figure 6 (429 m/s): initial lighter lines appear at the edge of the particles upon impact (t = 4.0 μs) that spread and expand up until t = 8.0 μs. As the cracks and open interfaces expand, the total volume occupied by the particles increases allowing for the particles to interact with one another. This provides the opportunity for additional stress concentrations as well as frictional heating, in addition to the potential for hot spots to form at crack tips.

The second set of samples contained two low defect HMX crystals laid out as in Figure 4. These crystals were placed again at the rear of the sample with about 10 mm of matrix material between the front of the sample and the crystals. The crystals contain far fewer initial defects than the production crystals and are notably larger. As expected, these experiments displayed less apparent cracking than the production-grade particles above, but still displayed evidence of damage, particularly at the crystal-crystal interface. In the same form as the multi-particle samples, each of these figures show a frame from directly before impact, another from when the compressive wave reaches the crystal, and a third from the maximum damage before the sample is removed from the viewing window. Figure 7 (443 m/s) shows the top portion of two crystals laid very closely together in the matrix with a thin line representing the interface between the crystals. Upon impact, straight light lines appear running from the bottom left to the top right, originating from the crystal-crystal interface.

In the third frame, the lines have expanded further into each crystal, particularly the back (right) crystal. In that final frame, the top right corner of the back crystal separates, pointing to the conclusion that these light lines are cracks and not just open interfaces due to debonding. In addition, the interface between the two crystals expands slightly. Figure 8 (488 m/s) shows some similar effects, although requires more explanation. The two crystals can be clearly seen before impact, but the lack of contrast causes the front crystal to primarily disappear in subsequent frames. The only trace of the front crystal left in the second and third frames is a network of straight light lines extending into the crystal, likely cracks originating at the crystal-crystal interface as discussed with Figure 7. The same crack network can be seen in the rear crystal, however when the reflected wave returns, the crystal appears to twist (t = 7.8 μs) and crack further before the sabot enters the frame. This reflected wave originates from a stress wave that is reflected off the steel disk at the rear of the sample due to the impedance mismatch between the PBX and back plate. The twisting motion likely results from either non-planar contact between the back of the crystal and the steel back plate, or a non-planar initial impact.

Figure 9 exhibited slightly different behavior than the other two. The second image in the sequence (t = 4.6 μs) shows the initial light lines, but this time more prominent in the forward crystal and more severe. The lines, however, are not as linear as figures 7 and 8, pointing to possible opening interfaces due to debonding between the crystal and matrix. A potential explanation for this debonding can be seen in the third frame at t = 8.0 μs as a clear separation be-

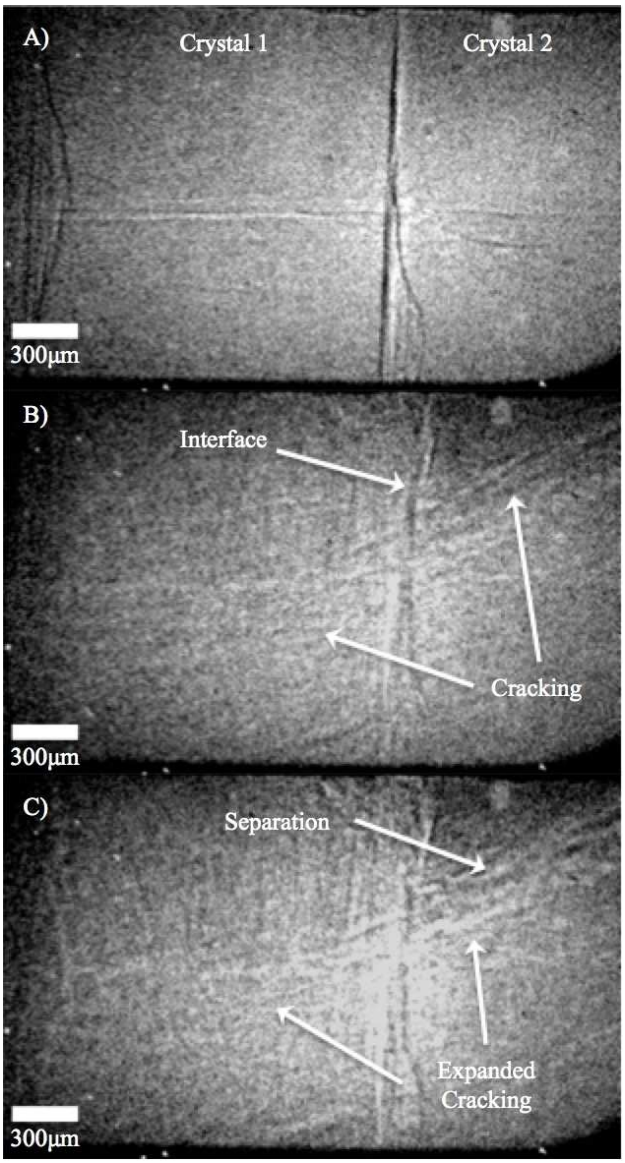

Figure 7. Image sequence of low defect HMX impacted at 443 m/s at A) 0 μs, B) 5.6 μs, and C) 9.0 μs.

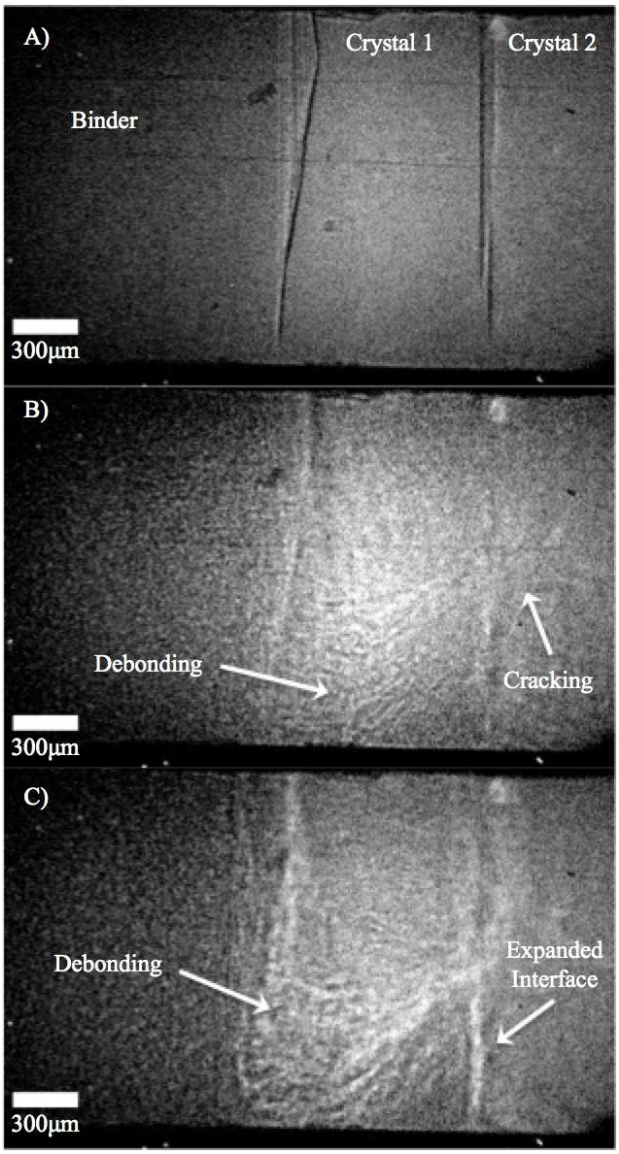

Figure 8. Image sequence of low defect HMX impacted at 488 m/s at A) 0 μs, B) 4.4 μs, and C) 7.8 μs.

comes apparent between the two crystals. This separation is more significant than that seen in other samples and is likely not entirely caused by the reflected wave. The separation of the crystals at their interface has two additional explanations. First, the expansion may be caused by the rotation of the crystals since the forward plane of the first crystal was not completely flat (similar to Figure 8, this time at the crystal-crystal interface rather than the back). The separation may also be caused by a reaction in the HMX crystals causing an expansion. As the crystals primarily separate after impact, increased stress concentrations are likely more influential than any frictional heating in this sample type (versus samples with many more particles present). Additionally, to help give an idea of the pressure in the samples, 1-D shock matching calculations were performed [15, 30]. While these are simplified and do not account for attenuation, it gives an estimate of approximately 1 GPa for the samples discussed in this paper.

4 Conclusions

Impact loading was applied to polymer-bonded HMX particles and crystals in rectangular geometries at impact velocities ranging from 420 to 488 m/s to observe their dynamic deformation and damage processes in real-time. A single-stage light gas gun was used to supply the dynamic load, and the high-speed deformation and damage were

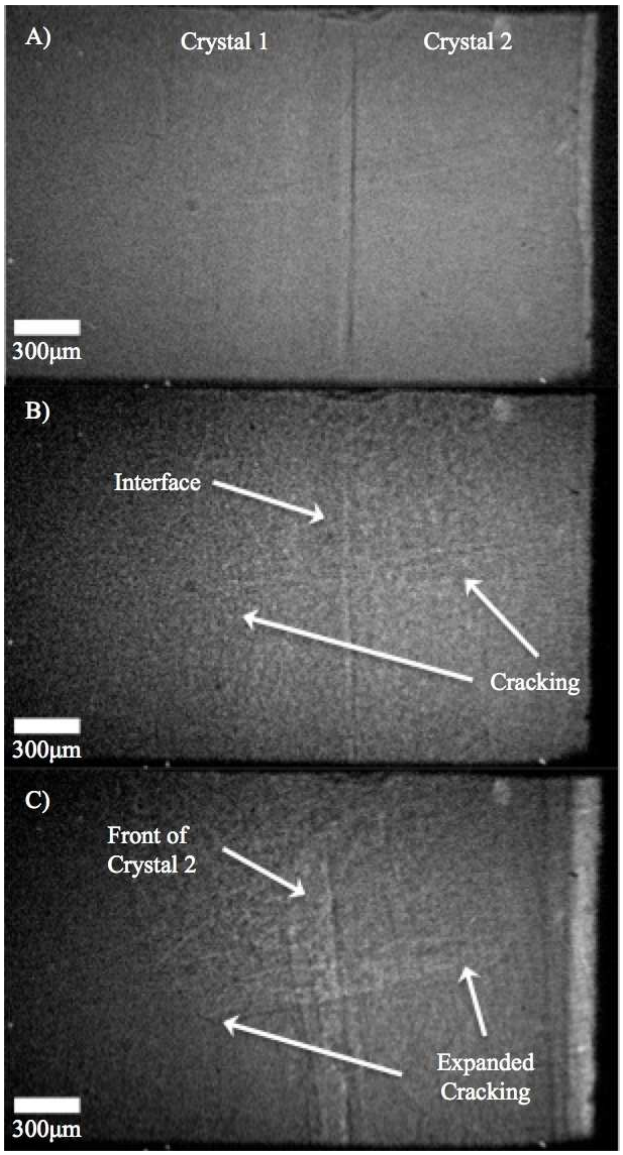

Figure 9. Image sequence of low defect HMX impacted at 432 m/s at A) 0 μs, B) 4.6 μs, and C) 8.0 μs.

captured by X-ray PCI at a frame rate of 5 MHz. These experiments provide the generation of the critical stress conditions that are necessary for reaction inside an HMX particle and the capturing of the dynamic behavior. The impact conditions were methodically adjusted in order to make progress towards determining a critical condition for the reaction. To this end, this study found that higher velocity is likely needed to see consistent evidence of hot spot formation and growth. An increase in impact velocity led to more fracture and intensified particle/matrix debonding. First, the multi-particle production samples showed significant damage as expected. Upon impact, expansion occurred from potential cracks and open interfaces causing the particles to expand. The initial lines formed at the particle edges before spreading throughout the entire crystal. Some of the lines forming at the edges appeared curve, likely pointing to open interfaces due to debonding, however, most appeared linear and spread through the sample, evidencing cracks. These samples acted similarly to the production-grade single particles previously examined (particle expansion due to cracking and open interfaces) [15], but at lower impact velocities, likely due to increased stress concentrations from the particle-particle interactions occurring as the particles expanded into one another (i.e. damage seen in single-particle experiments at 440 m/s was seen in multiple particle experiments at 400 m/s). For the two crystal samples, evidence of cracking was observed originating from the crystal-crystal interface, most often spanning from the bottom left to the top right. In the final frame of Figure 7, the top right corner of the rear crystal separated along these lighter lines, leading to the conclusion that these lines were in fact cracks. Figure 9 showed an increased separation at the crystal-crystal interface, leading to what appears to be debonding (indicated by curves lighter lines). This separation was likely either caused by wave mechanics or a possible reaction.

Acknowledgements

The authors would like to thank the Office of Naval Research as this research is funded through the project award N00014-16-1-2557 to Purdue University. They would also like to thank Benjamin J. Claus and Cody D. Kirk of Purdue University as well as Alex Deriy and Niranjan Parab of Argonne National Laboratory for their help in conducting the experiments. Additionally, funding for the equipment used in this work was provided by AFOSR Award No. FA9550-16-1-0315 (Dr. Martin Schmidt, Program Officer). Finally, use of the Advanced Photon Source, an Office of Science User Facility operated for the US Department of Energy (DOE) Office of Science by Argonee National Laboratory was supported by the US DOE under contract No. DE-AC02-06CH11357.

References

[1] T. Zhou, J. Lou, Y. Zhang, H. Song, F. Huang, Hot Spot Formation and Chemical Reaction Initiation in Shocked HMX Crystals with Nanovoids: A Large-Scale Reactive Molecular Dynamics Study, *Phys. Chem. Chem. Phys.* **2016**, *26*, 17627.

[2] A. K. Sikder, N. Sikder, A Review of Advanced High Performance, Insensitive and Thermally Stable Energetic Materials Emerging for Military and Space Applications, *J. Hazard. Mater.* **2004**, *112*, 1.

[3] C. S. Coffey, R. W. Armstrong, *Description of "hot spots" associated with localized shear zones in impact tests. In Shock Waves and High-Strain-Rate Phenomena in Metals*, . Springer, Boston, MA, **1981**, pp. 313–324.

[4] C. M. Tarver, S. K. Chidester, A. L. Nichols, Critical Conditions for Impact-and Shock-Induced Hot Spots in Solid Explosives, *J. Phys. Chem.* **1996**, *100*, 5794–5799.

[5] J. E. Field, N. K. Bourne, S. J. P. Palmer, S. M. Walley, Hot-Spot Ignition Mechanisms for Explosives and Propellants, *Philos. Trans. R. Soc. London Ser. A* **1992**, *339*, 269–283.

[6] R. N. Mulford, J. A. Romero, Sensitivity of the TATB-Based Explosive PBX-9502 after Thermal Expansion, *10th Conference of the American Physical Society Topical Group on Shock Compression of Condensed Matter,* Amherst, Massachusetts (USA), July 27 – August 1, **1997**, AIP Conference Proceedings 429, p. 723, DOI: https://doi.org/10.1063/1.55672.
[7] E. M. Hunt, S. Malcom, M. Jackson, High-Speed Study of Drop-Weight Impact Ignition of PBX 9501 Using Infrared Thermography, *ISRN Mechanical Engineering* **2011**, Article ID 872693, DOI: https://doi.org/10.5402/2011/872693 .
[8] D. N. Preston, P. D. Peterson, K. Y. Lee, D. E. Chavez, R. Deluca, G. Avilucea, S. Hagelberg, Effects of Damage on Non-Shock Initiation of HMX-Based Explosives, *APS Shock Compression of Condensed Matter Meeting Abstracts*, **2009**.
[9] N. K. Bourne, A. M. Milne, On Cavity Collapse and Subsequent Ignition, *12th Symposium (International) on Detonation,* San Diego, CA, USA, August 11 – 16, **2002**, pp. 213–219.
[10] Y. Q. Wu, F. L. Huang, Z. Y. Zhang, Experiments and Modeling of HMX Granular Explosives Subjected to Drop-Weight Impact, *RSC Adv*. **2012**, *2*, 4152.
[11] M. R. Baer, W. M. Trott, Mesoscale Descriptions of Shock-Loaded Heterogeneous Porous Materials, *12th Conference of the American Physical Society Topical Group on Shock Compression of Condensed Matter,* Atlanta, Georgia (USA), June 24 – 29, **2001**, AIP Conference Proceedings 620, p. 713, DOI: https://doi.org/10.1063/1.1483637.
[12] B. Tanasoiu, M. Koslowski, A Parametric Study of the Dynamic Failure of Energetic Composites, *J. Appl. Phys.* **2017**. *122*, 125103.
[13] J. K. Dienes, Frictional Hot-Spots and Propellant Sensitivity, *Mater. Res. Soc. Symp. Proc.* **1984**, *24*, 373–381.
[14] J. K. Dienes, Q. H. Zuo, J. D. Kershner, Impact Initiation of Explosives and Propellants via Statistical Crack Mechanics, *J. Mech. Phys. Solids* **2006**, *54*, 1237–1275.
[15] N. E. Kerschen, C. J. Sorensen, Z. Guo, J. O. Mares, K. Fezzaa, T. Sun, S. F. Son, W. W. Chen, X-ray Phase Contrast Imaging of the Impact of a Single HMX Particle in a Polymeric Matrix, *Propellants Explos. Pyrotech.* **2019**, *44*, 447.
[16] Y. M. Gupta, S. J. Turneaure, K. Perkins, K. Zimmerman, N. Arganbright, G. Shen, P. Chow, Real-Time, High-Resolution X-Ray Diffraction Measurements on Shocked Crystals at a Synchrotron Facility, *Rev. Sci. Instrum.* **2012**, *83*, 123905.
[17] W. W. Chen, M. C. Hudspeth, B. Claus, N. D. Parab, J. T. Black, K. Fezzaa, S. N. Luo, *In Situ* Damage Assessment Using Synchrotron X-Rays in Materials Loaded by a Hopkinson Bar, *Philos. Trans. R. Soc. A* **2014**, *372(215)*, 20130191, DOI: https://doi.org/10.1098/rsta.2013.0191.
[18] B. J. Jensen, S. N. Luo, D. E. Hooks, K. Fezzaa, K. J. Ramos, J. D. Yeager, K. Kwiatkowski, T. Shimada, D. M. Dattelbaum, Ultrafast, High Resolution, Phase Contrast Imaging of Impact Response with Synchrotron Radiation, *AIP Adv*. **2012**, *2*, 012170.
[19] M. Hudspeth, T. Sun, N. Parab, Z. Guo, K. Fezzaa, S. Luo, W. Chen, Simultaneous X-Ray Diffraction and Phase-Contrast Imaging for Investigating Material Deformation Mechanisms During High-Rate Loading, *J. Synchrotron Radiat.* **2015**, *22*, 49.
[20] S. N. Luo, B. J. Jensen, D. E. Hooks, K. Fezzaa, K. J. Ramos, J. D. Yeager, K. Kwiatkowski, T. Shimada, Gas Gun Shock Experiments with Single-Pulse X-Ray Phase-Contrast Imaging and Diffraction at the Advanced Photon Source, *Rev. Sci. Instrum.* **2012**, *83*, 073903.
[21] R. H. B. Bouma, A. G. Boluijt, H. J. Verbeek, A. E. D. M. Van der Heijden, On the Impact Testing of Cyclotrimethylene Trinitramine Crystals with Different Internal Qualities, *J. Appl. Phys.* **2008**, *103*, 93517.
[22] R. H. B. Bouma, W. Duvalois, A. E. D. M. Van der Heijden, and A. C. Van der Steen, Characterization of a Commercial-Grade CL-20: Morphology, Crystal Shape, Sensitivity, and Shock Initiation Testing by Flyer Impact*, 31st Int. Annual Conference of ICT*, Karlsruhe, Germany, June 27 – 30, **2000**.
[23] R. N. Mulford, J. A. Romero, Sensitivity of the TATB-based Explosive PBX-9502 after Thermal Expansion, *10th Conference of the American Physical Society Topical Group on Shock Compression of Condensed Matter,* Amherst, Massachusetts (USA), July 27 – August 1, **1997**, AIP Conference Proceedings 429, p. 723, DOI: https://doi.org/10.1063/1.55672.
[24] T. Zhou, J. Lou, Y. Zhang, H. Song, F. Huang, Hot Spot Formation and Chemical Reaction Initiation in Shocked HMX Crystals with Nanovoids: a Large-Scale Reactive Molecular Dynamics Study, *Phys. Chem. Chem. Phys.* **2016**, *18*, 1762.
[25] D. A. Varfolomeev, K. F. Grebenkin, A. L. Zherebtsov, M. V. Taranik, Hot Surfaces in Heterogeneous Explosives Initiated by a Shock Wave, *Combust. Explos. Shock Waves* **2010**, *46*, 482.
[26] G. Flowers, S. Switzer, Background Material Properties of Selected Silicone Potting Compounds and Raw Materials for their Substitute, 19MHSMP-78-18, **1978**, .
[27] N. D. Parab, Z. A. Roberts, M. H. Harr, J. O. Mares, A. D. Casey, I. E. Gunduz, M. Hudspeth, B. Claus, T. Sun, K. Fezzaa, S. F. Son, W. W. Chen, High Speed X-Ray Phase-Contrast Imaging of Energetic Composites under Dynamic Compression, *Appl. Phys. Lett.* **2016**, *109*, 131903.
[28] M. Nikl, Scintillation Detectors for X-Rays, *Meas. Sci. Technol.* **2006**, *17*, R37.
[29] T. Gureyev, S. Wilkins, On X-Ray Phase Imaging with a Point Source, *J. Opt. Soc. Am.* **1998**, *15*, 579–585.
[30] P. W. Cooper, Explosives Engineering, Wiley-VCH, Weinheim, Germany **1996**.

Manuscript received: June 25, 2019
Revised manuscript received: October 27, 2019
Version of record online: February 4, 2020

